AMERICAN SOCIETY FOR MICROBIOLOGY | Journal of Virology®

VIRUS-CELL INTERACTIONS

HPV-18E6 Inhibits Interactions between TANC2 and SNX27 in a PBM-Dependent Manner and Promotes Increased Cell Proliferation

Justyna Karolina Broniarczyk,[a,b] Paola Massimi,[a] Oscar Trejo-Cerro,[a] Michael P. Myers,[a] Lawrence Banks[a]

[a]International Centre for Genetic Engineering and Biotechnology, Padriciano, Trieste, Italy
[b]Department of Molecular Virology, Adam Mickiewicz University, Uniwersytetu Poznanskiego, Poznan, Poland

ABSTRACT Cancer-causing HPV E6 oncoproteins contain a PDZ-binding motif at the extreme carboxy terminus, which plays an important role in the viral life cycle and in the development of malignancy. Through this motif, HPV E6 targets a large number of cellular substrates, many of which are involved in processes related to the regulation of cell polarity. Recent studies also demonstrated E6's PDZ binding motif (PBM)-dependent association with SNX27, with a potential role in the perturbation of endocytic transport. Here, we have performed a proteomic analysis to identify SNX27-interacting partners whose binding to SNX27 is specifically perturbed in an E6-dependent manner. Extracts of HeLa cells that express GFP-tagged SNX27, transfected with control siRNA or siRNA targeting E6AP, were subject to GFP immunoprecipitation followed by mass spectroscopy, which identified TANC2 as an interacting partner of SNX27. Furthermore, we demonstrate that HPV E6 inhibits association between SNX27 and TANC2 in a PBM-dependent manner, resulting in an increase in TANC2 protein levels. In the absence of E6, SNX27 directs TANC2 toward lysosomal degradation. TANC2, in the presence of HPV-18E6, enhances cell proliferation in a PBM-dependent manner, indicating that HPV E6 targets the SNX27-mediated transport of TANC2 to promote cellular proliferation.

IMPORTANCE While a great deal is known about the role of the E6 PDZ binding motif (PBM) in modulating the cellular proteins involved in regulating cell polarity, much less is known about the consequences of E6's interactions with SNX27 and the endocytic sorting machinery. We reasoned that a potential consequence of such interactions could be to affect the fate of multiple SNX27 endosomal partners, such as transmembrane proteins or soluble accessory proteins. Using a proteomic approach in HPV-18-positive cervical tumor-derived cells, we demonstrate that TANC2 is an interacting partner of SNX27, whose interaction is blocked by E6 in a PBM-dependent manner. This study therefore begins to shed new light on how E6 can regulate the endocytic transport of multiple SNX27-binding proteins, thereby expanding our understanding of the functions of the E6 PBM.

KEYWORDS HPV, E6, TANC2, SNX27, endocytic transport

Human papillomaviruses (HPVs) are small nonenveloped DNA viruses that cause nearly 5% of all human malignancies. These viruses are responsible for the development of a range of different malignancies, of which cervical cancer is the most important, causing more than 500,000 cases and 250,000 deaths annually (1 to 3). While over 200 different HPV types have been identified, only a small subset is cancer-causing, with the most prevalent being HPV-16 and HPV-18 (3, 4).

HPVs induce malignancy largely through the action of two viral oncoproteins, E6 and E7. Both proteins play essential roles in the viral life cycle, creating an environment within the differentiating epithelium favorable to replication of the viral genome. This is brought about through perturbation of normal cell cycle control pathways and an induction of an S-phase-like state, through the actions of E7 in targeting a plethora of

Editor Lori Frappier, University of Toronto

Address correspondence to Justyna Karolina Broniarczyk, justekbr@amu.edu.pl, or Lawrence Banks, banks@icgeb.org.
The authors declare no conflict of interest.

Received 1 September 2022
Accepted 4 October 2022
Published 3 November 2022

cell cycle regulators, including the pRb family of pocket proteins (5). The normal cellular response to this deregulation of the cell cycle is a p53-dependent apoptotic response (6), which is overcome through the action of the E6 oncoprotein and the subsequent degradation of p53 in an E6AP-dependent manner (7). For reasons that still remain unclear, in individuals the viral infection remains persistent over many months and years, changes are initiated that ultimately result in the development of malignancy. Common to all of these cases is a continued high-level expression of E6 and E7, which continues to drive subsequent tumor development. However, loss of function or reduced expression of either oncoprotein is sufficient to block continued tumor development, and cells either enter senescence or undergo apoptosis (8, 9). Thus, both viral oncoproteins remain excellent targets for therapeutic intervention in HPV-induced malignancy.

Although the targeting pf pRB family members and p53 are essential features of cancer progression, other functions of the viral oncoproteins are also critical to this process. In the case of cancer-causing HPV E6 oncoproteins, the PDZ binding motif (PBM) at its carboxy terminus, which is absent from the E6s of benign HPV types, appears to be particularly important (10, 11). This motif confers interaction with cellular proteins that contain PDZ domains (Post Synaptic Density-95 [PSD-95], Discs-Large [DLG1] and Zonula Occludens 1 [ZO-1]), of which there are over 200 in the human proteome (12). Several cellular PDZ domain-containing substrates of the different high-risk HPV E6 oncoproteins have been identified (13), and many of these appear to be associated with pathways controlling cell polarity and include Discs Large (DLG1) and Scribble (hScrib) (14).

Interestingly, recent studies identified a novel function of the E6 PBM and linked this to the regulation of endocytic transport pathways (15). High-risk HPV E6s were found to interact with sorting nexin 27 (SNX27), an essential component of the retromer complex, which controls the correct trafficking of many different cargos, including transmembrane receptors, transporters, ion channels, solute carriers, and soluble signaling and regulatory proteins (16, 17). It has been found that at least one such cargo, GLUT1, is aberrantly trafficked as a result of the E6 PBM-dependent interaction with SNX27. Moreover, it has been shown that, unlike most of its PDZ domain-containing targets, E6 does not target SNX27 for degradation. Instead, in HPV-18-positive cell lines, the association of SNX27 with components of the retromer complex and the endocytic transport machinery is altered in an E6 PBM-dependent manner (15). Proteomic studies have also indicated that E6 could potentially interact with other components of the retromer complex, including Vps35, Vps26, and Vps29 (18), although whether these interactions are the result of the association of E6 with SNX27 remains to be determined.

While a great deal is known about the cargoes that can be potentially transported by SNX27, it is noteworthy that many of these studies have been performed in HeLa cells where there is high-level expression of HPV-18 E6, which could potentially modulate the pattern of SNX27-cargo interactions (16). We were therefore interested in analyzing how loss of E6 might alter the pattern of SNX27-binding proteins in HeLa cells and thereby shed further light on the biological relevance of this association. In this study, we identify TANC2 as an interacting partner of SNX27, whose interaction with SNX27 is specifically blocked in an E6 PBM-dependent manner, which contributes toward enhanced levels of proliferation in HPV-positive cells.

RESULTS

Identification of TANC2 as an interacting partner of SNX27. Previous studies had shown that HPV E6 interacts with SNX27 and can potentially perturb the normal endosomal trafficking of certain cargoes (15). Since earlier proteomic analysis of the SNX27 interactome had been performed in HeLa cells (16), we wanted to analyze directly how this might be modulated by the endogenous HPV-18 E6 present within these cells. To do this, we first generated a HeLa cell line stably expressing GFP-SNX27, and, as can be seen from Fig. 1A, this is expressed in a punctate manner typical of the normal pattern of SNX27 expression (16). Using this cell line as a basis, we then transfected the cells

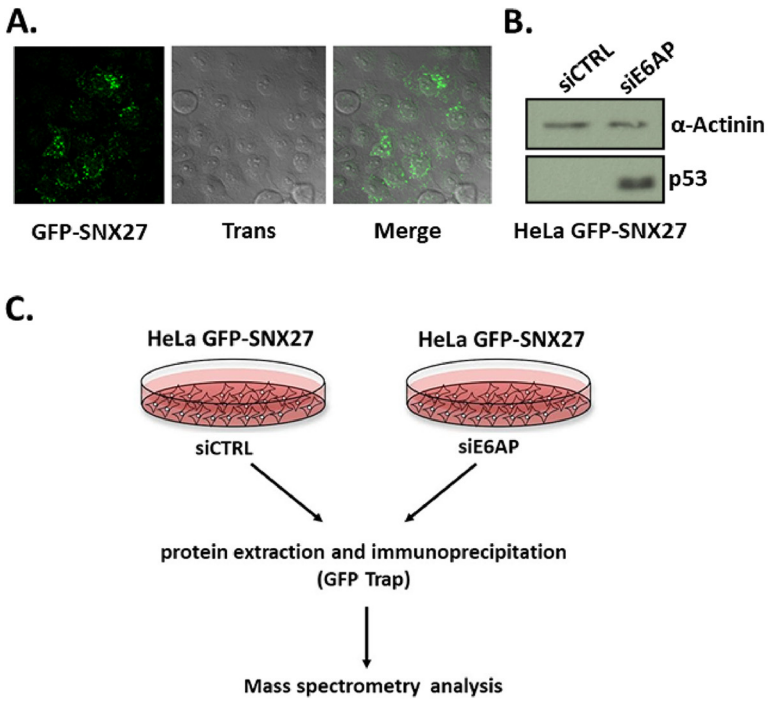

D.

Identification of Tanc2 as a prominent SNX27 hit in HeLa stable expressing GFP-SNX27, treated with siRNA E6AP

Protein	PBM motif X S/T X L/V	Log(e)	Log(l)	%/%	# of peptides	Total
SNX27	-	-155.1	7.61	9.3/12	15	38
Tanc2	ESNV	-27.2	6.02	3.7/6	5	5

FIG 1 Identification of TANC2 as an interacting partner of SNX27. (A) To generate a HeLa cell line stably expressing GFP-SNX27, HPV-18-positive HeLa cells were transfected with a GFP-SNX27-expressing plasmid and subjected to G418 selection over 2 weeks. Representative pictures of HeLa stably expressing SNX27 are shown. (B) Western blot analysis of HeLa stably expressing GFP-SNX27, transfected with control siRNA and siRNA targeting E6AP, confirmed the silencing of 18E6 protein. (C) Protein extracts from HeLa stably expressing GFP-SNX27, transfected with control siRNA and siRNA targeting E6AP, were immunoprecipitated with GFP-Trap, and the immunoprecipitated material was analyzed by mass spectroscopy. (D) The table shows identification of TANC2 as the prominent SNX27 hit in HeLa stably expressing GFP-SNX27, transfected with E6AP siRNA, together with E value (the base-10 log of the expectation that the assignment is stochastic), L value (the base −10 log of the sum of the intensities of the fragment ion spectra), protein coverage (% of protein residues/% corrected for unlikely peptides), the number of unique peptide sequences (#), and total number of tandem mass spectra that can be assigned to each protein.

with siRNA scrambled as a control, or siRNA E6AP, which has been shown previously to very effectively abolish expression of the E6 oncoprotein (19). Silencing of 18E6 was confirmed by Western blotting using the p53 antibody, using increased p53 levels as a surrogate marker for E6 silencing (Fig. 1B). After 72 h, the cells were harvested and immunoprecipitated using anti-GFP antibody-conjugated agarose beads (GFP-trap) to pull down SNX27 and any associated proteins. The samples were then subjected to mass spectrometry analysis (Fig. 1C). The resulting protein profiles were compared with those obtained from control and siRNA E6AP-treated cells, with our focus being on those proteins that contain a PBM. The most striking candidate in this analysis was TANC2. This is a canonical carboxy-terminal PBM-containing protein that was only detected in the absence of E6, indicating that this is a potential interacting partner of SNX27 whose association is blocked by the presence of E6 (Fig. 1D). In addition, these

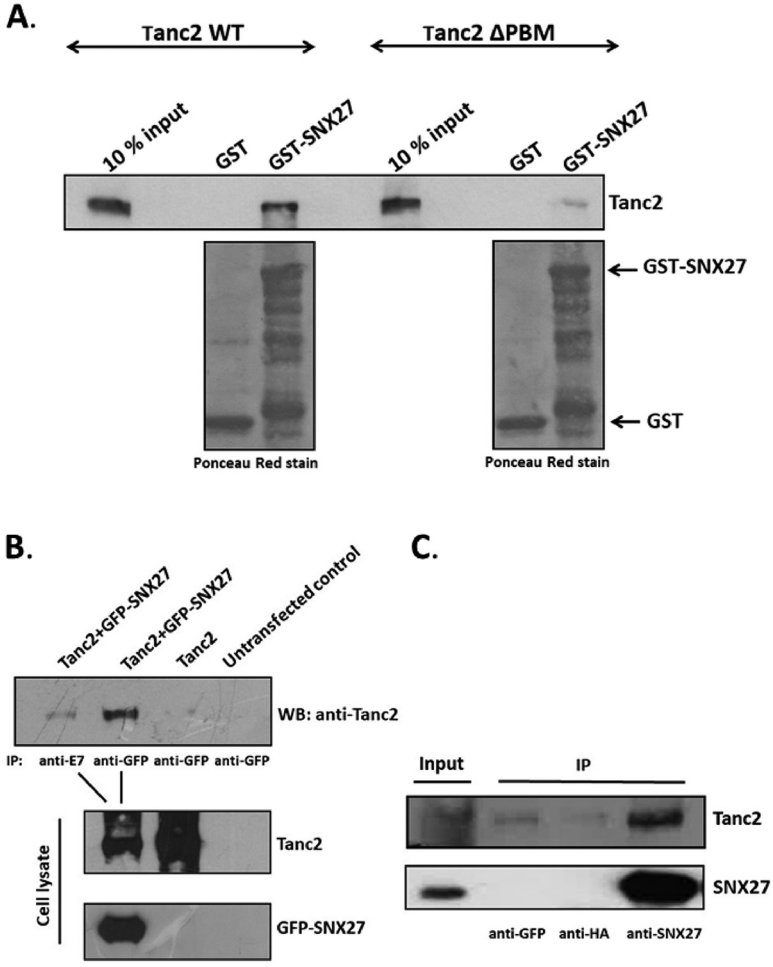

FIG 2 TANC2 interacts with SNX27 *in vitro* and *in vivo*. (A) A GST-pulldown assay using GST alone or GST-SNX27, incubated with extracts of HEK293 cells transfected with plasmids expressing TANC2 WT or ΔPBM. Western blot analysis of the bound proteins shows that TANC2 binding to SNX27 is PBM dependent (upper panel). The lower panel shows the Ponceau Red-stained membrane. (B) HEK293 cells were transfected with plasmids expressing GFP-SNX27 and TANC2, or GFP-SNX27 alone. As control, untransfected cells were used. After 24 h, cell extracts were immunoprecipitated using rabbit anti-GFP antibody and protein A-conjugated Sepharose beads. As a control, lysates from cells transfected with plasmids expressing GFP-SNX27 and TANC2 were divided and immunoprecipitated using either rabbit anti-GFP or rabbit anti-E7 (unrelated) antibody. Coimmunoprecipitating TANC2 was then detected by Western blotting using mouse anti-TANC2 antibody (upper panel). (C) HEK293 cells were transfected with plasmid expressing TANC2 alone. After 24 h, the cell extracts were immunoprecipitated using mouse anti-SNX27 antibody and protein G-conjugated Sepharose beads. As control, lysates from cells transfected with plasmids expressing TANC2 alone were divided and immunoprecipitated, using either mouse anti-GFP or mouse anti-HA (unrelated) antibodies. Coimmunoprecipitating TANC2 was then detected by Western blotting using rabbit anti-TANC2 antibody (upper panel).

results confirm previous findings in which TANC2 was identified in the mass spectrometric analysis of SNX27 cellular partners in HPV-negative RPE1 (human retinal pigment epithelial-1) cells (16). Moreover, SNX27 and TANC2 interactions were also found in a recently described PDZ–PBM interactome analysis (20). To determine whether TANC2 binds SNX27 in a PBM-dependent manner, we analyzed whether TANC2 and SNX27 can associate *in vitro* and *in vivo*. To do this, wild type and a PBM deletion mutant of TANC2 (ΔPBM) were overexpressed in HEK293 cells; the cell extracts were used in a pulldown assay with the GST-SNX27 fusion protein, and the bound proteins were analyzed by immunoblotting using an anti-TANC2 antibody. As can be seen from Fig. 2A, TANC2 interacts with SNX27 in a PBM-dependent manner. To confirm that TANC2 and SNX27 also interact *in vivo*, we used a coimmunoprecipitation assay. HEK293 cells were transfected with the TANC2-expressing plasmid alone or in combination with plasmid

expressing GFP-tagged SNX27. After 24 h, the cells were harvested and cell extracts immunoprecipitated with rabbit anti-GFP antibody or, as a control, with rabbit anti-E7 antibody. Coimmunoprecipitating TANC2 was then detected by Western blotting using mouse anti-TANC2 antibody. The results in Fig. 2B demonstrate a clear interaction between TANC2 and SNX27. To further confirm the interaction, the assay was repeated using HEK293 cells transfected only with TANC2-expressing plasmid. Similarly, after 24 h, the cells were harvested, and cell extracts were immunoprecipitated with mouse anti-SNX27 antibody or, as a control, with mouse anti-GFP and anti-HA antibodies. Coimmunoprecipitating TANC2 was then detected by Western blotting using a rabbit anti-TANC2 antibody. The results in Fig. 2C confirm the binding of TANC2 to endogenous SNX27.

HPV-18E6 inhibits interactions between TANC2 and SNX27 in a PBM-dependent manner. Having established that SNX27 and TANC2 interact in a PBM-dependent manner, we next sought to determine whether this was affected by the presence of HPV-18 E6. To do this, we again performed a glutathione S-transferase (GST) pulldown assay where SNX27, expressed as a GST fusion protein, and GST alone were incubated with cell extracts of HEK293 cells, either untransfected (control) or transfected with plasmids expressing HA-tagged HPV-18 E6 wild type (WT). The results shown in Fig. 3A confirm that E6 also binds GST-SNX27 and show that the presence of HPV-18 E6 inhibits TANC2 binding to GST-SNX27. We repeated this analysis using extracts from HeLa cells in the presence (siCTRL) and absence of E6 (siE6AP), and, as can be seen from Fig. 3B, E6 again binds strongly to SNX27, as would be expected, and TANC2 interaction with SNX27 is stronger in the absence of E6. Finally, in order to demonstrate that this inhibitory effect of E6 occurs via its PBM, the pulldown assay was repeated using cells expressing HPV-18 E6, either wild type or the T156E mutant (whose PBM is nonfunctional). As can be seen from Fig. 3C, loss of the E6 PBM reduces E6's association with SNX27 and at the same time allows association between SNX27 and TANC2. Taken together, these results indicate that TANC2 is a PBM-dependent interacting partner of SNX27 and that their association is inhibited by HPV-18 E6 in a PBM-dependent manner.

The stability of TANC2 and HPV E6 are regulated in a PBM-dependent manner. Having shown that HPV-18 E6 can inhibit the association between TANC2 and SNX27, we wanted to determine how this might be reflected in changes to the levels of TANC2 protein. To do this, HeLa cells were transfected with siRNA E6AP in order to knock down HPV E6 (19) and control siRNA, and the levels of TANC2 were analyzed by Western blotting. As can be seen from Fig. 4A, loss of E6/E6AP induced a marked decrease in the levels of TANC2. In order to determine whether this loss is SNX27 dependent, cells were knocked down for SNX27 alone and doubly knocked down for E6AP and SNX27; as can be seen from Fig. 4A, loss of SNX27 has no major effect on TANC2 levels in HeLa cells.

To confirm that TANC2 protein levels can be stabilized by E6 in cells other than HeLa cells, we repeated the experiment using HPV-18-positive C4-1 cells and HPV-16-positive SiHa and CaSki cell lines. These cell lines were transfected with either scrambled siRNA as a control or siRNA E6AP to knock down HPV E6 protein (19), and the levels of TANC2 in the cell lysates were analyzed by Western blotting. As can be observed in Fig. 4B, loss of E6 significantly decreased TANC2 levels in all HPV-positive cells tested, suggesting that both HPV-18 and HPV-16 E6 oncoproteins can regulate TANC2 stability. Since it was possible that TANC2 levels were regulated directly by E6AP, rather than by E6, we performed similar experiments using HPV-negative C33A and HaCaT cells, transfected with scrambled siRNA as a control and siRNA E6AP. The Western blotting results in Fig. 4B show that loss of E6AP does not affect TANC2 levels in HPV-negative cell lines, confirming that TANC2 levels are regulated by HPV E6 protein, rather than by E6AP.

Having established that HPV-18E6 inhibits the interactions between TANC2 and SNX27 in a PBM-dependent manner, we sought to verify how this might be reflected in changes to the levels of TANC2 and E6 proteins. First, to determine whether TANC2 levels might be affected by HPV-18E6 in a PBM-dependent manner, we overexpressed TANC2 in HEK293 cells in the presence of HPV-18E6 wild type or the 18E6T156E PBM mutant, defective for PDZ domain binding. Western blot analysis confirms that the TANC2 levels are stabilized

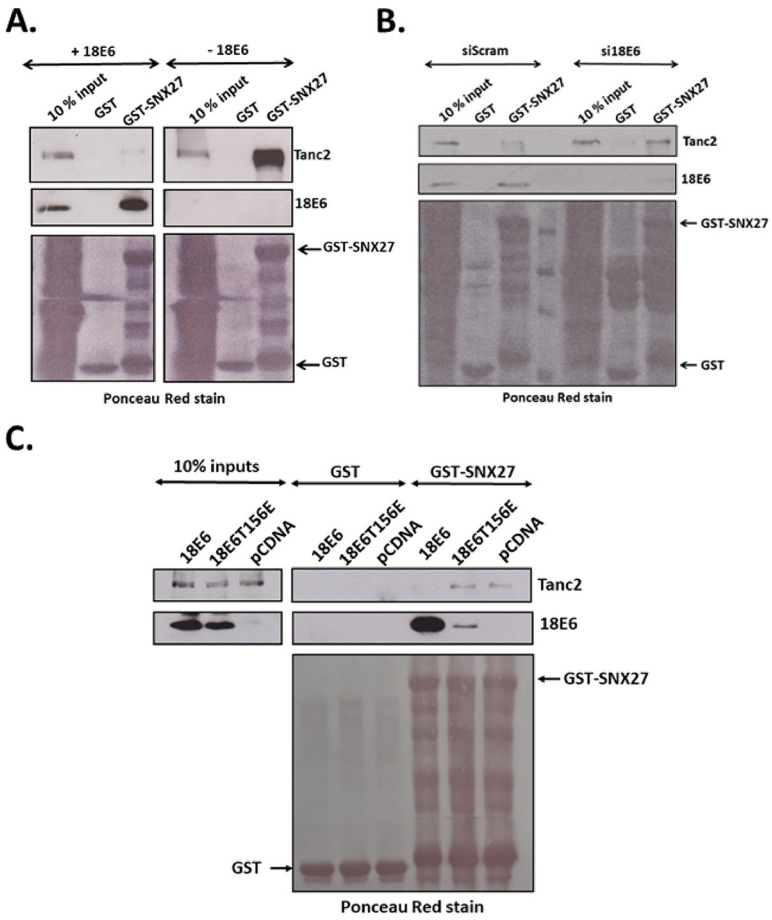

FIG 3 HPV-18E6 inhibits interactions between TANC2 and SNX27 in a PBM-dependent manner. (A) A GST-pulldown assay using GST alone or GST-SNX27, incubated with the extracts of HEK293 cells transfected with plasmids expressing HA-tagged HPV-18 E6 wild type (WT). Western blotting was used to assess the levels of endogenous TANC2 or exogenous HA-E6 bound to the GST fusion proteins. Note that TANC2 binding to GST-SNX27 is inhibited by the presence of HPV-18 E6 and that E6 also binds GST-SNX27. (B) The GST-pulldown assay was repeated using extracts from HPV-18-positive HeLa cells treated for 72 h with siRNAE6AP to ablate E6 expression. Western blot analysis shows that the endogenous E6 in HeLa cells treated with siRNA scrambled (siScram) binds strongly to GST-SNX27, while TANC2 binding is low. Upon ablation of E6 (siRNA E6AP), TANC2 binding increases markedly. (C) The assay was repeated, including the HA-tagged HPV-18 E6T156E PBM mutant. Binding of E6T156E mutant to SNX27 is reduced dramatically, and its presence does not block TANC2-SNX27 binding, indicating the PBM-dependence of this interaction.

by HPV-18 E6 in a PBM-dependent manner (Fig. 4C). Next, to determine whether TANC2 can affect HPV-18E6 levels, we repeated the experiment, transfecting HEK293 cells with 18E6 WT or 18E6ΔPBM mutant alone or in the presence of TANC2. Interestingly, as can be seen in Fig. 4D, TANC2 appears to increase 18E6 levels in a PBM-dependent manner.

Ablation of HPV E6 directs TANC2 for lysosomal degradation. To determine whether the decrease in TANC2 levels in the absence of E6/E6AP was due to lysosomal degradation, the assay was repeated in the presence of the lysosome inhibitor chloroquine. As can be seen from Fig. 5A, a clear rescue of TANC2 is seen in the presence of chloroquine, indicating that association with SNX27 promotes the sorting of TANC2 into a pathway leading to lysosomal degradation. To further confirm this observation, we performed immunofluorescence analysis of TANC2 in HeLa cells transfected with siRNA scrambled (siCTRL) and siRNA E6AP. As can be seen from Fig. 5B, loss of E6/E6AP, as would be expected, increases TANC2 accumulation within lysosomal compartments. However, there is also a significant accumulation of TANC2 within the nucleus, the significance of which remains to be determined.

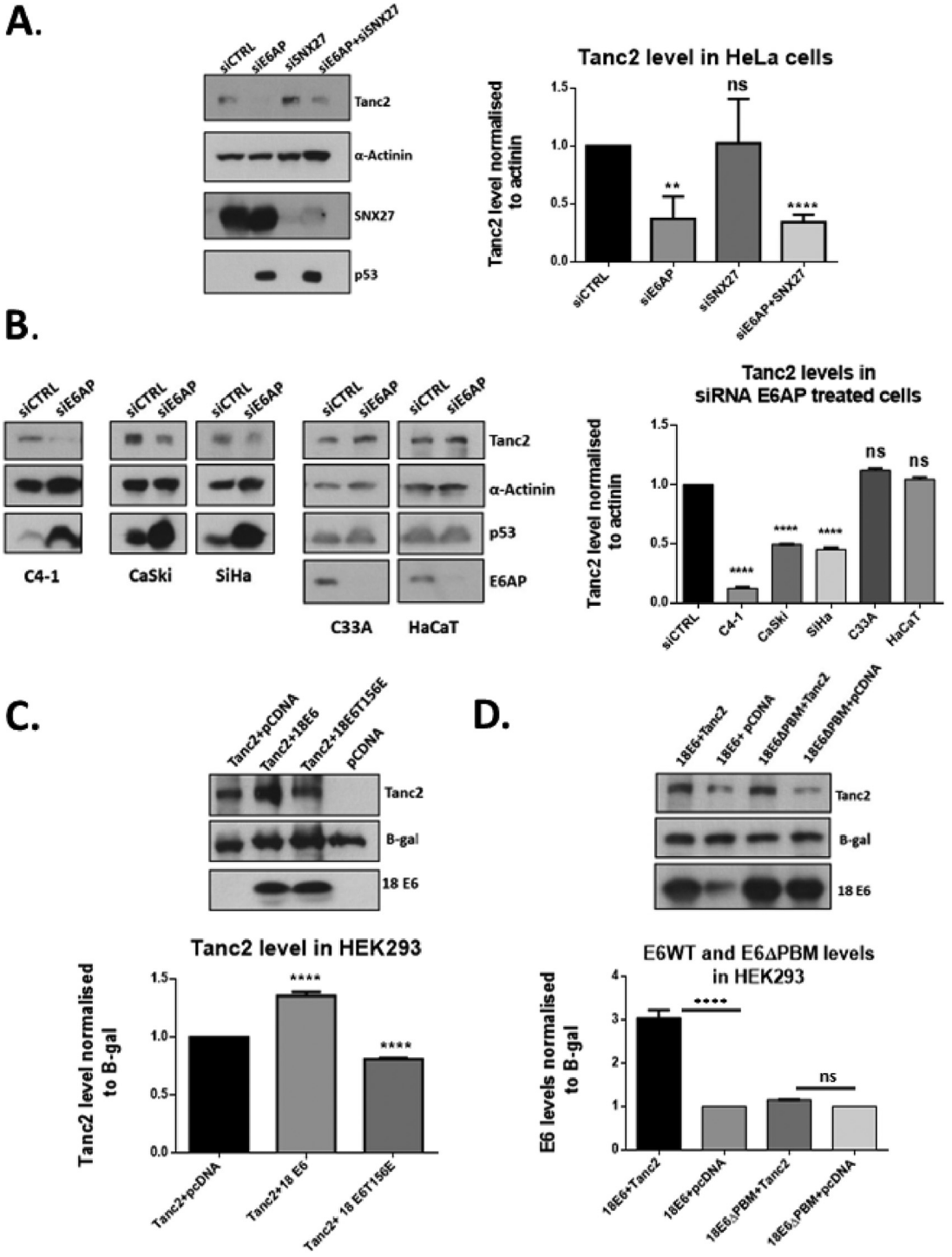

FIG 4 The stability of TANC2 and HPV E6 are regulated in a PBM-dependent manner. (A) HeLa cells were transfected with scrambled siRNA as a control, siRNA E6AP to silence 18E6, and siRNA SNX27. After 72 h, cells were harvested and total protein levels were detected by Western blotting with anti-TANC2 antibody and anti-SNX27 antibody, plus anti-p53 antibody to confirm E6 silencing and anti-α-actinin antibody to monitor protein loading. The upper panel shows representative images of the Western blot analyses. The lower panel shows quantification of TANC2 levels, normalized to α-actinin. The results are expressed as the means from at least three independent experiments, and the standard deviations are shown (**, $P < 0{,}01$; ****, $P < 0{,}0001$; ns, nonsignificant). (B) HPV-18-positive C4-1 cells, HPV-16-positive SiHa and CaSki, and HPV-negative C33A and HaCaT cells were transfected with scrambled siRNA as a control and siRNA E6AP. After 72 h, cells were harvested and total protein levels were detected by Western blotting with anti-TANC2 antibody, anti-p53 antibody to confirm E6 silencing, and anti-α-actinin antibody to monitor protein loading. The upper panel shows representative images of the Western blot analyses. The lower panels show quantification of TANC2 levels, normalized to α-actinin. The results are expressed as the

(Continued on next page)

TANC2 promotes cell proliferation in the presence of HPV-18E6 in a PBM-dependent manner. The *TANC2* gene was first reported as an oncogene in breast cancer cells, in which knockdown of the *TANC2* gene resulted in decreased cell viability (21). We were therefore interested in investigating whether knocking down TANC2 protein levels could affect the viability of cervical cancer cells. To do this, HPV-18-positive HeLa cells and HPV-negative C33A cells were transfected with siRNA TANC2, or siRNA scrambled as a control. After 72 h, the cells were trypsinized, collected, and counted. The silencing of TANC2 was confirmed by Western blotting. As shown in Fig. 6A, silencing of TANC2 expression results in a 50% reduction in HeLa cell numbers but has no effect upon HPV-negative C33A cell numbers. These data indicate that loss of TANC2 expression in HeLa cells results in a reduction in total cell numbers.

In order to further confirm that E6's blocking of SNX27-mediated transport of TANC2 can result in increased levels of proliferation, we performed a colony-forming assay in C33A cells in the presence of ectopically expressed TANC2 and HPV-18 E6 WT or HPV-18 E6ΔPBM mutant. The cells were transfected with empty vector or plasmid expressing TANC2, either alone or in combination with plasmids expressing HPV-18E6 WT or HPV-18 E6ΔPBM mutant. The cells were then subjected to Hygromycin B selection, after which the colonies were stained with Giemsa stain and counted. The results shown in Fig. 6B indicate that overexpression of TANC2 in the presence of HPV-18E6 drastically increases the formation of colonies compared with cells expressing either HPV-18E6 or TANC2 alone. Interestingly, we did not observe any increase in the number of colonies when TANC2 is overexpressed in the presence of HPV-18 E6ΔPBM mutant, suggesting that TANC2 promotes the proliferation of cervical tumor-derived cells in the presence of HPV E6 and that this process is regulated in a PBM-dependent manner.

DISCUSSION

Human papillomaviruses induce malignancy through the action of the E6 and E7 viral oncoproteins, and both are required for the development and maintenance of the cancer phenotype. Despite the years of research on E6 and E7, there are still gaps in our understanding of how they work, both to facilitate the normal life cycle of the virus and in their contribution to malignancy (22).

Many steps in carcinogenesis—loss of cell polarity, dynamic changes in cell morphology, and increased cell motility and invasion—are regulated by the endocytic transport machinery (23). Moreover, SNX27, which mediates a variety of protein–protein interactions important in trafficking, protein sorting, and membrane remodelling, is increasingly associated with carcinogenesis (24), affecting tumor growth *in vitro* and *in vivo* (25 to 27). However, the molecular mechanisms through which SNX27 contributes to different cancer cells remains unclear. While E6 has been shown to affect endocytic transport of GLUT1 through its association with SNX27 (15), little is known about any other endocytically controlled signaling pathways that might be affected.

To investigate which components of the trafficking pathway might be affected by the SNX27-HPV E6 interaction, we generated a HeLa cell line expressing GFP-SNX27 and analyzed its SNX27 proteome interaction profile in the presence or absence of HPV E6. Mass spectrometry identified a number of SNX27-interacting proteins, of which the most striking was TANC2. This PBM protein, detected only in the absence of E6, is involved in cell growth

FIG 4 Legend (Continued)
means from at least three independent experiments, and the standard deviations are shown (****, $P < 0{,}0001$; ns, nonsignificant). (C) TANC2, alone, or with HA-18E6 or HA-18E6T156E (PBM mutant, which is defective for PDZ domain binding), was expressed in HEK293 cells. After 48 h, cell lysates were collected and analyzed by Western blotting, using the following antibodies: α-TANC2, α-β-Galactosidase, and α-HA to detect HPV-18 E6. The left panel shows representative images of the Western blot analyses. The right panel shows quantification of TANC2 levels, normalized to β-Galactosidase. The results are expressed as the means from at least three independent experiments, and the standard deviations are shown (****, $P < 0{,}0001$). (D) GFP-18E6 or GFP-18E6ΔPBM mutant alone or in the presence of TANC2 were expressed in HEK293 cells. After 48 h, cell lysates were collected and analyzed by Western blotting, using the following antibodies: α-TANC2, α-β-Galactosidase, and α-E6 to detect HPV-18 E6. The right panel shows quantification of E6 levels, normalized to β-Galactosidase and relative to GFP-18E6 or GFP-18E6ΔPBM alone. The results are expressed as the means from at least three independent experiments, and the standard deviations are shown (****, $P < 0{,}0001$; ns, nonsignificant).

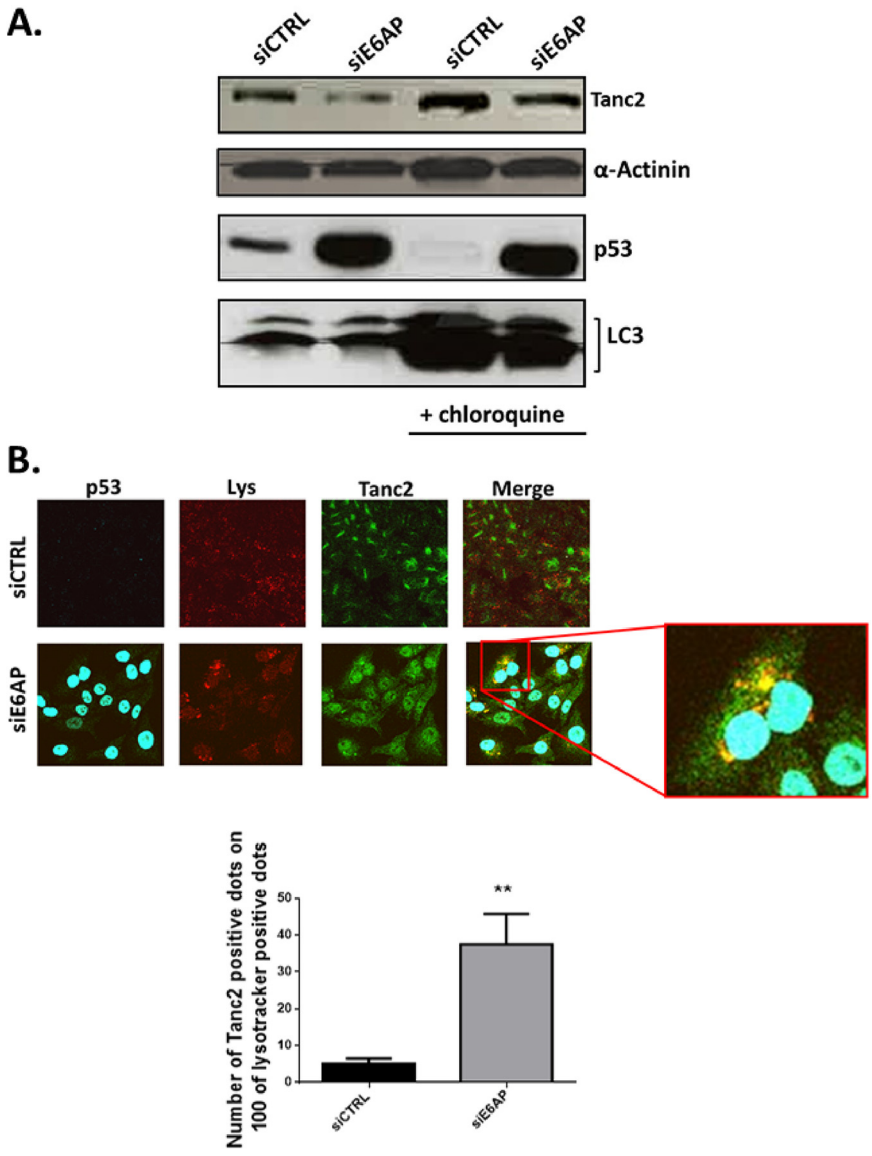

FIG 5 Ablation of E6 directs TANC2 toward lysosomal degradation. (A) HeLa cells were transfected with scrambled siRNA as control or siRNA E6AP to knock down E6 expression After 48 h, cells were incubated with or without chloroquine then harvested 24 h later. The total protein levels were detected by Western blotting with anti-TANC2 antibody, anti-p53 antibody to confirm E6 silencing, and anti-α actinin antibody to monitor protein loading. (B) HeLa cells were transfected with scrambled siRNA (siCTRL) or siRNA E6AP. After 72 h, cells were stained with Lysotracker (red) followed by immunolabeling of TANC2 (green) and p53 (far red). Representative images are shown (left panel). Quantification of TANC2 distribution within lysosome compartments is also shown (right panel), based on the number of TANC2-positive dots on 100 Lysotracker-positive dots. The results are expressed as the means from at least three independent experiments, and the standard deviations are shown (**, $P < 0{,}01$).

and survival and is believed to play an important role in carcinogenesis in a context-dependent manner (21), indicating that it might be an important E6 target that is normally regulated by SNX27. Indeed, TANC2 had been previously identified in the mass spectrometric analysis of SNX27 cellular partners in HPV-negative RPE1 (human retinal pigment epithelial-1) cells and in the recently described PDZP–BM interactome analysis (16). However, to our knowledge, no TANC2–SNX27 interaction had ever been verified biochemically.

Here, we confirm that SNX27 interacts *in vitro* and *in vivo* with TANC2 in a PBM-dependent manner, and that E6 competes with TANC2 for SNX27 binding. As a consequence, loss of E6/E6AP in HPV-positive cells induces a marked decrease in TANC2 levels, while loss of

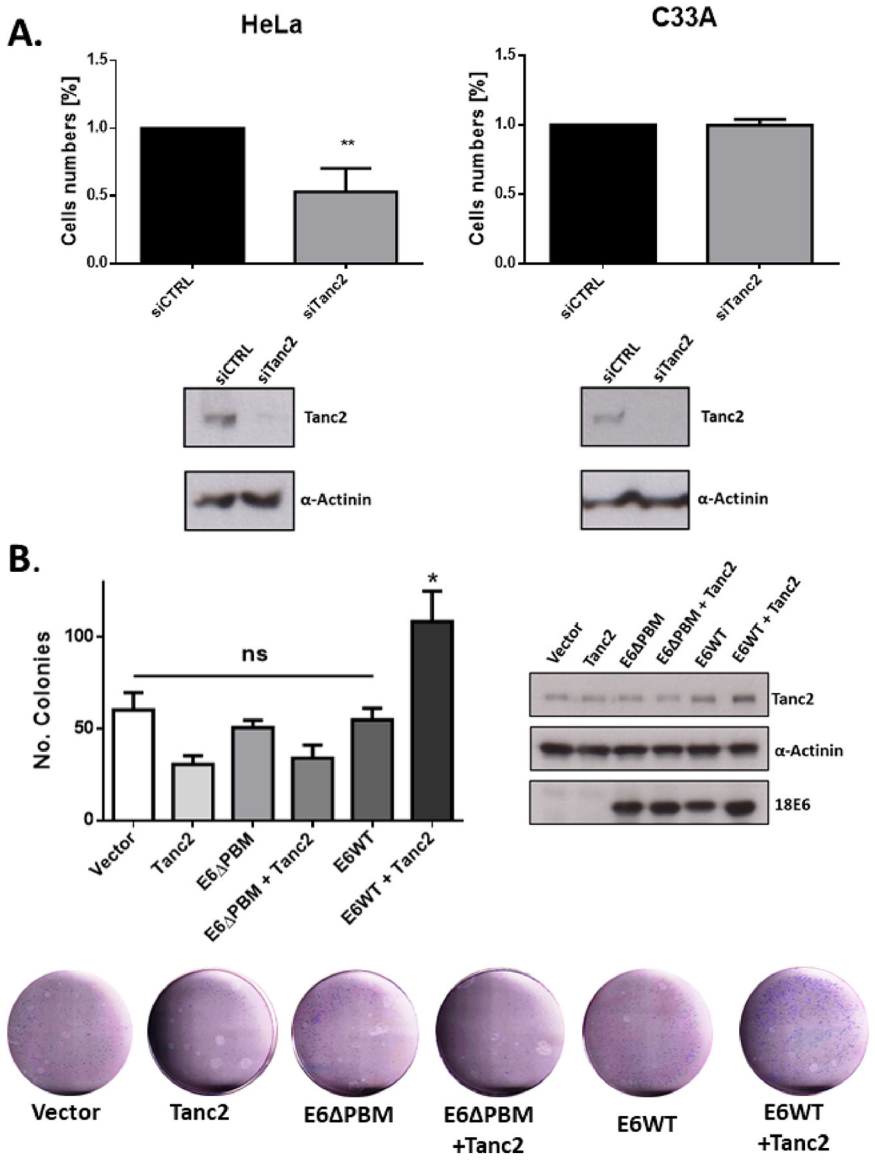

FIG 6 TANC2 promotes cell proliferation in the presence of HPV-18E6 in a PBM-dependent manner. (A) HeLa and C33A cells were transfected with control siRNA (siCTRL) or siRNA specifically targeting TANC2. Seventy-two hours after transfection, the cells were trypsinized, collected, and counted using a hemacytometer. The number of cells in siTANC2-treated samples was normalized to the number of cells in siCTRL-treated samples in each experiment. Histograms show the cell numbers, expressed as means from at least three independent experiments, and the standard deviations are shown (**, $P < 0,01$). The silencing of TANC2 was confirmed by Western blotting (right panels). Note that loss of TANC2 correlates with reduced cell numbers in HPV-18-positive HeLa cells. (B) C33A cells were seeded at low confluence and transfected after 24 h with plasmids expressing HPV-18E6 or HPV-18E6ΔPBM in the presence or absence of TANC2 and selected for 14 to 21 days with Hygromycin B. Colonies were fixed and stained with Giemsa and counted using the software Plot Histograms of Colony Size (countPHICS). Representative pictures are shown in the upper left panel, and quantification of the colony formation rate is shown in the lower left panel. The results are expressed as means from at least three independent experiments, and the standard deviations are shown (*, $P < 0,1$; ns, nonsignificant). The expression of HPV-18E6, HPV-18E6ΔPBM, and TANC2 were confirmed by Western blotting (right panels). Note that overexpression of TANC2 in the presence of HPV-18E6 drastically increases the formation of colonies compared with cells expressing TANC2 and HPV-18E6ΔPBM together or TANC2 and HPV-18E6 alone.

SNX27 does not. Although the use of a pool E6AP siRNAs might increase the probability of off-target effects, no decrease in TANC2 levels is seen in E6AP-ablated HPV-negative cells, indicating that the effect is HPV E6 specific. In addition, the stability of both TANC2 and HPV E6 were shown to be regulated in a PBM-dependent manner.

A previous analysis of the surface proteome of SNX27- and VPS35-depleted HeLa cells showed TANC2 to be unaffected (16), which is consistent with our findings, as TANC2 is not a transmembrane protein but is a soluble SNX27-binding regulatory protein (17). Additionally, recent studies have identified SNX27 high- and low-affinity ligands, based on the amino acid sequences upstream of the PBM motif. High-affinity cargoes require acidic residues located at −3 and −5 positions that clamp a conserved arginine on the SNX27 surface. In contrast, TANC2, based on the sequence of its C terminus motif (pkrPFvESnV), belongs to class 3a ligands that bind relatively weakly to SNX27 (17).

To examine the potential mechanisms for the reduced TANC2 levels in HPV-18 E6-ablated HeLa cells, we blocked lysosomal degradation using chloroquine, which resulted in dramatic increases in TANC2 levels in the presence or absence of E6, indicating that TANC2 levels are regulated through the lysozome. Indeed, immunofluorescence analysis showed increased TANC2 accumulation within lysosomal compartments in HPV-18 E6-ablated HeLa cells. Intriguingly we also observed some TANC2 accumulation in the nucleus in the same analysis. Previous studies have indeed indicated a possible interaction of TANC2 with nucleus receptors and nuclear transport machinery (28), and this may be a reflection of a possible increase in these associations. However, significantly more work will be required to understand the relevance of this observation in the context of HPV E6.

Previous studies had shown that loss of TANC2 decreases the viability of breast cancer cells and induces apoptosis (21). In HPV-18-positive, but not HPV-negative, cervical cancer cells, we found that ablation of TANC2 reduces cell numbers, while ectopic expression of E6 and TANC2 dramatically increases colony formation in HPV-negative cells, apparently in a PBM-dependent manner. However, since the levels of E6 are also higher in cells overexpressing TANC2, we cannot at this stage specify whether the increase in the number of colonies is due to an E6-TANC2-specific function or is simply a reflection of increased levels of E6.

These data raise a number of questions concerning the mechanism(s) by which TANC2 modulates cell proliferation. Although *TANC2* has been identified as an oncogene in breast cancer cells (21), the role of TANC2 in carcinogenesis in general is not yet understood; little is known about TANC2-interacting proteins, or about the signaling pathways that it might affect, potentially leading to cancer development. *In silico* analysis suggested that TANC2 functions in several biological processes: the canonical WNT pathway, the noncanonical WNT/planar cell polarity pathway, in Rap2-mediated signaling, and in the HIPPO pathway (28). All of these pathways have been documented to control cancer cell proliferation, migration, and survival. Therefore, it is probable that alterations in TANC2's cellular distribution and levels might affect them and could contribute to cancer development.

Previous studies have shown that at least one SNX27 cargo, the glucose transporter GLUT1, is aberrantly trafficked due to the E6 PBM-dependent interaction with SNX27. Here, we demonstrate that HPV-18E6 inhibits interactions between TANC2 and SNX27 in a PBM-dependent manner and that HPV-18E6 blocks TANC2's lysosomal degradation, resulting in faster proliferation and growth of tumor cells. Thus, the interplay between these proteins may play an important role in maintaining the tumorigenic phenotype of the cancer cells. Taken together, these studies confirm that PBM-containing HPV E6 oncoproteins can modulate endosomal transport and that this novel activity of E6 may contribute to cancer development.

MATERIALS AND METHODS

Plasmids. pGWI HA-18E6WT and pGWI HA-18E6T156E, which is defective for PDZ domain binding, have been described previously (29, 30). pHAHA-empty GFP and pHAHA-GFP18E6 were made by subcloning green fluorescent protein (GFP) from peGFP C1 plasmid (Addgene, #6084-1) using NheI and BamHI restriction sites into the pHAHA empty vector (Addgene, #12617) (31) and were kindly provided by Arushi Vats. The pHAHA-Empty GFP plasmid was used to clone 18E6. To make pHAHA-GFP18E6, 18E6 sequence was first amplified from the pEGFP-18E6 plasmid, using EcoRI and SalI restriction sites, and then cloned into the pHAHA-GFP vector. The primer sequences used are as follows: GFP18E6_F: ATA

GAA TTC ATG GCG CGC TTT GAG GAT C and GFP18E6_R: CCT GTC GAC TTA TAC TTG TGT TTC TCT GC. The p3xFlag-Tanc2WT construct was kindly provided by Eunjoon Kim and has been described previously (32). The p3xFlag-Tanc2ΔPBM and pHAHA-GFP18E6ΔPBM plasmids were generated using the Invitrogen Gene Tailor site-directed mutagenesis system and verified by sequencing. Oligonucleotides were designed in house and were synthesized by Eurofins Genomics. Constructs expressing GST-tagged SNX27 and GFP-tagged SNX27 were kindly provided by Martin P. Playford and have been described previously (33).

Cells and transfection. HeLa (ATCC) and GFP-SNX27 HeLa cells were maintained in Dulbecco's Modified Eagle's Medium (DMEM), supplemented with 10% fetal calf serum (Life Technology), penicillin-streptomycin (100 U/mL), and glutamine (300 μg/mL). Cells were cultured at 37°C with 10% CO_2. To generate a HeLa cell line stably expressing GFP-SNX27, HPV-18-positive HeLa cells were transfected with a GFP-SNX27-expressing plasmid and subjected to G418 selection over 2 weeks. After this time, single-cell clones were picked and then analyzed by Western blotting for GFP-SNX27 using mouse anti-GFP antibody (Santa Cruz).

HeLa and C33A cells were transfected with siRNA using Lipofectamine RNAiMAX transfection reagent (Invitrogen). The following siRNA Smart Pools from Dharmacon were used: E6AP, SNX27, and TANC2, while the scrambled siSTABLE nontargeting siRNA was used as control. For HEK293 cell transfections, calcium phosphate precipitation was used, as described previously (34).

Mass spectrometry analysis. HeLa cells stably expressing GFP-SNX27 were transfected with a control siRNA or siRNA E6AP to reduce levels of HPV-18E6 expression. After 72 h, the cells were extracted in mass spectrometry lysis buffer (50 mM HEPES, pH 7.4, 150 mM NaCl, 50 mM NaF, 1 mM EDTA, 0.25% NP-40) and incubated with GFP Trap (Chromotek) for 2 to 3 h on a rotating wheel at 4°C. The beads were then extensively washed, and the samples were subjected to mass spectroscopic analysis, as previously described (35). The interacting partners of SNX27 were compared between control and siRNA E6AP-treated cells. Briefly, proteins were eluted directly from the affinity beads using 50 ng of sequencing grade trypsin (Promega) in 20 mM diammonium phosphate pH 8.0, for 6 h at 37°C. The supernatant was removed from the beads, and the cysteines were reduced and alkylated by boiling for 2 min in the presence of 10 mM Tris (2-carboxyethyl) phosphine (Pierce), followed by incubation with 20 mM acetaminophen (Sigma) for 1 h at 37°C. The reactions were stopped by the addition of acetic acid (Sigma) to 0.1%. The resulting mixture was desalted using C18 Ziptips (Millipore) and lyophilized to dryness. Nanobore columns were constructed using Picofrit columns (NewObjective) packed with 15 cm of 1.8 mm Zorbax XDB C18 particles, using a home-made high-pressure column loader. The desalted samples were injected onto the nanobore column in buffer A (10% methanol/0.1% formic acid). The column was developed with a discontinuous gradient and sprayed directly into the orifice of an LTQ ion trap mass spectrometer (Thermo Electron). A cycle of one full scan (400 to 1700 *m/z*), followed by eight data-dependent MS/MS scans at 25% normalized collision energy, was performed throughout the LC separation. RAW files from the LTQ were converted to mzXML files by rEADW (version 1.6) and searched against the Ensembl human protein database.

Glutathione S-transferase (GST) pulldown assay. GST-tagged fusion proteins were expressed and purified as described previously (36). HEK293 cells were harvested and lysed in RIPA buffer (20 mM Tris pH 7.5, 150 mM NaCl, 1 mM EDTA, 1 mM EGTA, 1% Triton X-100) containing protease inhibitors (Calbiochem Protease Cocktail 1). The extracts were clarified by centrifugation and then incubated with the SNX27 GST fusion proteins for 2 h at room temperature. After extensive washing, the bound proteins were analyzed by SDS-PAGE and Western blotting.

Coimmunoprecipitation assay. HEK293 cells were transfected with plasmids expressing GFP-SNX27 and TANC2, or GFP-SNX27 alone, for 24 h. As a control, nontransfected cells were used. After 24 h, the cells were harvested in RIPA buffer containing protease inhibitors (Calbiochem Protease Cocktail 1). Cell extracts were immunoprecipitated using rabbit anti-GFP antibody (Abcam) and protein A-conjugated Sepharose beads. As a control, lysates from cells transfected with plasmids expressing GFP-SNX27 and TANC2 were divided and immunoprecipitated using rabbit anti-GFP or rabbit anti-E7 (unrelated) antibody. Coimmunoprecipitating TANC2 was then detected by Western blotting using mouse anti-TANC2 antibody. The assay was repeated using HEK293 cells transfected with plasmid expressing TANC2 alone. After 24 h, the cells were harvested, and cell extracts were immunoprecipitated using mouse anti-SNX27 antibody and protein G-conjugated Sepharose beads. As a control, lysates from cells transfected with plasmids expressing TANC2 alone were divided and immunoprecipitated using either mouse anti-GFP (Santa Cruz) or mouse anti-HA (unrelated) antibodies. Coimmunoprecipitating TANC2 was then detected by Western blotting using rabbit anti-TANC2 antibody (upper panel).

Immunofluorescence assay. HeLa cells were seeded on glass coverslips at a density of approximately 1.2×10^5 cells/coverslip and transfected with siRNA scrambled as control or siRNA E6AP. After 72 h, cells were stained with Lysotracker (Invitrogen) following the manufacturer's protocol and then fixed with 4% paraformaldehyde and permeabilized by PBS/0.1% Triton X-100. Immunostaining was performed by incubating the coverslips in PBS containing antibodies against TANC2 (Abcam) and p53 (Santa Cruz), as indicated, overnight in a humidified chamber at 4°C. The coverslips were then washed thrice with PBS and incubated with the appropriate fluorophore-conjugated secondary antibodies, as indicated, for 1 h in a humidified chamber at 37°C. The coverslips were then washed thrice with PBS and twice with distilled water and mounted onto glass slides. The images were captured using the LSM510 META Confocal microscope (Carl Zeiss).

Proliferation assay. C33A and HeLa cells were plated in a 12-well plate, incubated for 24 h, and transfected with siRNA specifically targeting TANC2 or with a control siRNA (siCTRL). After 72 h, the cells were trypsinized, collected, and counted using a hemocytometer. The numbers of cells in siTANC2-treated samples were normalized to the numbers of cells obtained for siCTRL-treated samples in each experiment. Western blotting of the cellular lysates was also used to confirm the efficiency of TANC2 silencing by TANC2 or CTRL siRNAs, as indicated.

Colony formation assay. C33A cells were seeded in 6-cm^2 plates at low confluence (15,000 cells/dish). After 24 h, cells were transfected with a TANC2-expressing plasmid, together with plasmids expressing either HPV-18E6 WT, HPV-18E6ΔPBM, or a control plasmid, and were selected for 14 to 21 days with Hygromycin B (Invitrogen). Colonies were then stained with Giemsa stain (1% crystal violet, 25% methanol) and counted using the software Plot Histograms of Colony Size (countPHICS) (37). Each experiment was repeated a minimum of 3 times.

Statistical analysis. All experiments were performed with appropriate repetitions. Statistical significance was calculated using the GraphPad Prism 6 software.

ACKNOWLEDGMENTS

We are most grateful to Miranda Thomas for her valuable comments on the manuscript. We express our thanks to Arushi Vats, Eunjoon Kim, and Martin P. Playford for kindly providing plasmids. This work was supported by a research grant from the Associazione Italiana per la Ricerca sul Cancro (Progetto IG 2019 ID 23572.). J.K.B. gratefully acknowledges support from the Umberto Veronesi Foundation (postdoctoral fellowship, years 2018, 2020, and 2022).

REFERENCES

1. IARC working group on the evaluation of carcinogenic risks to humans. 2012. Biological agents. IARC Monogr Eval Carcinog Risks Hum 100:1–441.
2. Parkin DM, Bray F. 2006. Chapter 2: the burden of HPV-related cancers. Vaccine 24:S11–S25. https://doi.org/10.1016/j.vaccine.2006.05.111.
3. zur Hausen H. 2009. Papillomaviruses in the causation of human cancers—a brief historical account. Virology 384:260–265. https://doi.org/10.1016/j.virol.2008.11.046.
4. Bouvard V, Baan R, Straif K, Grosse Y, Secretan B, El Ghissassi F, Benbrahim-Tallaa L, Guha N, Freeman C, Galichet L, Cogliano V, WHO International Agency for Research on Cancer Monograph Working Group. 2009. A review of human carcinogens—Part B: biological agents. Lancet Oncol 10:321–322. https://doi.org/10.1016/s1470-2045(09)70096-8.
5. Munger K, Werness BA, Dyson N, Phelps WC, Harlow E, Howley PM. 1989. Complex formation of human papillomavirus E7 proteins with the retinoblastoma tumor suppressor gene product. EMBO J 8:4099–4105. https://doi.org/10.1002/j.1460-2075.1989.tb08594.x.
6. Scheffner M, Werness BA, Huibregtse JM, Levine AJ, Howley PM. 1990. The E6 oncoprotein encoded by human papillomavirus types 16 and 18 promotes the degradation of p53. Cell 63:1129–1136. https://doi.org/10.1016/0092-8674(90)90409-8.
7. Scheffner M, Huibregtse JM, Vierstra RD, Howley PM. 1993. The HPV-16 E6 and E6-AP complex functions as a ubiquitin-protein ligase in the ubiquitination of p53. Cell 75:495–505. https://doi.org/10.1016/0092-8674(93)90384-3.
8. DeFilippis RA, Goodwin EC, Wu L, DiMaio D. 2003. Endogenous human papillomavirus E6 and E7 Proteins Differentially Regulate Proliferation, Senescence, and Apoptosis in HeLa Cervical Carcinoma Cells. J Virol 77:1551–1563. https://doi.org/10.1128/jvi.77.2.1551-1563.2003.
9. Mittal S, Banks L. 2017. Molecular mechanisms underlying human papillomavirus E6 and E7 oncoprotein-induced cell transformation. Mutat Res Rev Mutat Res 772:23–35. https://doi.org/10.1016/j.mrrev.2016.08.001.
10. Ganti K, Broniarczyk J, Manoubi W, Massimi P, Mittal S, Pim D, Szalmas A, Thatte J, Thomas M, Tomaic V, Banks L. 2015. The human papillomavirus E6 PDZ binding motif: from life cycle to malignancy. Viruses 7:3530–3551. https://doi.org/10.3390/v7072785.
11. Thomas M, Banks L. 2021. The biology of papillomavirus PDZ associations: what do they offer papillomaviruses? Curr Opin Virol 51:119–126. https://doi.org/10.1016/j.coviro.2021.09.011.
12. Nardella C, Visconti L, Malagrinò F, Pagano L, Bufano M, Nalli M, Coluccia A, La Regina G, Silvestri R, Gianni S, Toto A. 2021. Targeting PDZ domains as potential treatment for viral infections, neurodegeneration and cancer. Biol Direct 16:15. https://doi.org/10.1186/s13062-021-00303-9.
13. Thomas M, Myers MP, Massimi P, Guarnaccia C, Banks L. 2016. Analysis of multiple HPV E6 PDZ interactions defines type-specific PDZ fingerprints that predict oncogenic potential. PLoS Pathog 12:e1005766. https://doi.org/10.1371/journal.ppat.1005766.
14. Banks L, Pim D, Thomas M. 2012. Human tumour viruses and the deregulation of cell polarity in cancer. Nat Rev Cancer 12:877–886. https://doi.org/10.1038/nrc3400.
15. Ganti K, Massimi P, Manzo-Merino J, Tomaic V, Pim D, Playford MP, Lizano M, Roberts S, Kranjec C, Doorbar J, Banks L. 2016. Interaction of the human papillomavirus E6 oncoprotein with sorting nexin 27 modulates endocytic cargo transport pathways. PLoS Pathog 12:e1005854. https://doi.org/10.1371/journal.ppat.1005854.
16. Steinberg F, Gallon M, Winfield M, Thomas EC, Bell AJ, Heesom KJ, Tavaré JM, Cullen PJ. 2013. A global analysis of SNX27-retromer assembly and cargo specificity reveals a function in glucose and metal ion transport. Nat Cell Biol 15:461–471. https://doi.org/10.1038/ncb2721.
17. Clairfeuille T, Mas C, Chan AS, Yang Z, Tello-Lafoz M, Chandra M, Widagdo J, Kerr MC, Paul B, Merida I, Teasdale RD, Pavlos NJ, Anggono V, Collins BM. 2016. A molecular code for endosomal recycling of phosphorylated cargos by the SNX27-retromer complex. Nat Struct Mol Biol 23:921–932. https://doi.org/10.1038/nsmb.3290.
18. Rozenblatt-Rosen O, Deo RC, Padi M, Adelmant G, Calderwood MA, Rolland T, Grace M, Dricot A, Askenazi M, Tavares M, Pevzner SJ, Abderazzaq F, Byrdsong D, Carvunis A-R, Chen AA, Cheng J, Correll M, Duarte M, Fan C, Feltkamp MC, Ficarro SB, Franchi R, Garg BK, Gulbahce N, Hao T, Holthaus AM, James R, Korkhin A, Litovchick L, Mar JC, Pak TR, Rabello S, Rubio R, Shen Y, Singh S, Spangle JM, Tasan M, Wanamaker S, Webber JT, Roecklein-Canfield J, Johannsen E, Barabási A-L, Beroukhim R, Kieff E, Cusick ME, Hill DE, Münger K, Marto JA, Quackenbush J, Roth FP, et al. 2012. Interpreting cancer genomes using systematic host network perturbations by tumour virus proteins. Nature 487:491–495. https://doi.org/10.1038/nature11288.
19. Tomaić V, Pim D, Banks L. 2009. The stability of the human papillomavirus E6 oncoprotein is E6AP dependent. Virology 393:7–10. https://doi.org/10.1016/j.virol.2009.07.029.
20. Gogl G, Zambo B, Kostmann C, Cousido-Siah A, Morlet B, Durbesson F, Negroni L, Eberling P, Jane P, Nomine Y, Zeke A, Østergaard S, Monsellier E, Vincentelli R, Trave G. 2021. Quantitative fragmentomics allow affinity mapping of interactomes. bioRxiv. https://doi.org/10.1101/2021.10.22.465449.
21. Mahmood SF, Gruel N, Chapeaublanc E, Lescure A, Jones T, Reyal F, Vincent-Salomon A, Raynal V, Pierron G, Perez F, Camonis J, Del Nery E, Delattre O, Radvanyi F, Bernard-Pierrot I. 2014. A siRNA screen identifies RAD21, EIF3H, CHRAC1, and TANC2 as driver genes within the 8q23, 8q24.3, and 17q23 amplicons in breast cancer with effects on cell growth, survival and transformation. Carcinogenesis 35:670–682. https://doi.org/10.1093/carcin/bgt351.
22. Vats A, Trejo-Cerro O, Thomas M, Banks L. 2021. Human papillomavirus E6 and E7: what remains? Tumour Virus Res 11:200213. https://doi.org/10.1016/j.tvr.2021.200213.
23. Goldenring JR. 2013. A central role for vesicle trafficking in epithelial neoplasia: intracellular highways to carcinogenesis. Nat Rev Cancer 13:813–820. https://doi.org/10.1038/nrc3601.
24. Chandra M, Kendall AK, Jackson LP. 2021. Toward understanding the molecular role of SNX27/retromer in human health and disease. Front Cell Dev Biol 9:642378. https://doi.org/10.3389/fcell.2021.642378.
25. Zhang J, Li K, Zhang Y, Lu R, Wu S, Tang J, Xia Y, Sun J. 2019. Deletion of sorting nexin 27 suppresses proliferation in highly aggressive breast cancer MDA-MB-231 cells in vitro and in vivo. BMC Cancer 19:555. https://doi.org/10.1186/s12885-019-5769-z.
26. Sharma P, Parveen S, Shah LV, Mukherjee M, Kalaidzidis Y, Kozielski AJ, Rosato R, Chang JC, Datta S. 2020. SNX27–retromer assembly recycles MT1-MMP to invadopodia and promotes breast cancer metastasis. J Cell Biol 219:e201812098. https://doi.org/10.1083/jcb.201812098.

27. Yang L, Tan W, Yang X, You Y, Wang J, Wen G, Zhong J. 2021. Sorting nexins: a novel promising therapy target for cancerous/neoplastic diseases. J Cell Physiol 236:3317–3335. https://doi.org/10.1002/jcp.30093.
28. Gasparini A, Tosatto SCE, Murgia A, Leonardi E. 2017. Dynamic scaffolds for neuronal signaling: in silico analysis of the TANC protein family. Sci Rep 7:6829. https://doi.org/10.1038/s41598-017-05748-5.
29. Pim D, Thomas M, Javier R, Gardiol D, Banks L. 2000. HPV E6 targeted degradation of the discs large protein: evidence for the involvement of a novel ubiquitin ligase. Oncogene 19:719–725. https://doi.org/10.1038/sj.onc.1203374.
30. Thatte J, Massimi P, Thomas M, Boon SS, Banks L. 2018. The human papillomavirus E6 PDZ binding motif links DNA damage response signaling to E6 inhibition of p53 transcriptional activity. J Virol 92:e00465-18. https://doi.org/10.1128/JVI.00465-18.
31. Luu HH, Zhou L, Haydon RC, Deyrup AT, Montag AG, Huo D, Heck R, Heizmann CW, Peabody TD, Simon MA, He TC. 2005. Increased expression of S100A6 is associated with decreased metastasis and inhibition of cell migration and anchorage independent growth in human osteosarcoma. Cancer Lett 229:135–148. https://doi.org/10.1016/j.canlet.2005.02.015.
32. Han S, Nam J, Li Y, Kim S, Cho SH, Cho YS, Choi SY, Choi J, Han K, Kim Y, Na M, Kim H, Bae YC, Choi SY, Kim E. 2010. Regulation of dendritic spines, spatial memory, and embryonic development by the TANC family of PSD-95-interacting proteins. J Neurosci 30:15102–15112. https://doi.org/10.1523/JNEUROSCI.3128-10.2010.
33. Valdes JL, Tang J, McDermott MI, Kuo JC, Zimmerman SP, Wincovitch SM, Waterman CM, Milgram SL, Playford MP. 2011. Sorting nexin 27 protein regulates trafficking of a p21-activated kinase (PAK) interacting exchange factor (β-Pix)-G protein-coupled receptor kinase interacting protein (GIT) complex via a PDZ domain interaction. J Biol Chem 286:39403–39416. https://doi.org/10.1074/jbc.M111.260802.
34. Graham FL, van der Eb AJ. 1973. A new technique for the assay of infectivity of human adenovirus 5 DNA. Virology 52:456–467. https://doi.org/10.1016/0042-6822(73)90341-3.
35. Tomaić V, Gardiol D, Massimi P, Ozbun M, Myers M, Banks L. 2009. Human and primate tumour viruses use PDZ binding as an evolutionarily conserved mechanism of targeting cell polarity regulators. Oncogene 28:1–8. https://doi.org/10.1038/onc.2008.365.
36. Thomas M, Massimi P, Jenkins J, Banks L. 1995. HPV-18 E6 mediated inhibition of p53 DNA binding activity is independent of E6 induced degradation. Oncogene 10:261–268.
37. Brzozowska B, Gałecki M, Tartas A, Ginter J, Kaźmierczak U, Lundholm L. 2019. Freeware tool for analysing numbers and sizes of cell colonies. Radiat Environ Biophys 58:109–117. https://doi.org/10.1007/s00411-018-00772-z.